



# Superconducting Phases in Neutron Star Cores

Group Meeting  
Nov 27, 2020

Dr. Vanessa Graber  
Institute of Space Sciences

**ICE**

- Detailed BCS calculations provide the pairing gaps  $\Delta$ , which are associated with the **critical temperatures**  $T_c$  for the superfluid and superconducting phase transitions.

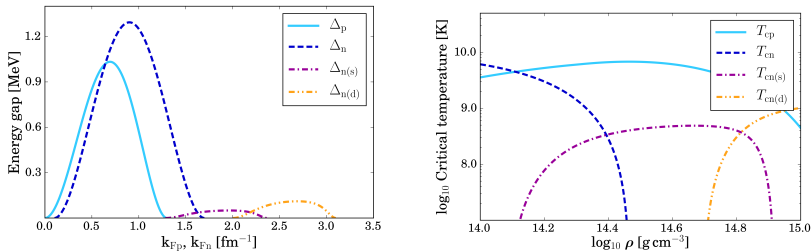


Figure 1: Left: Parametrised proton (singlet) and neutron (singlet, triplet) energy gaps as a function of Fermi wave numbers (Ho, Glampedakis & Andersson, 2012). Right: Critical temperatures of superconductivity/superfluidity as a function of the neutron star density. The values are computed for the NRAPR equation of state (Steiner et al., 2005; Chamel, 2008).

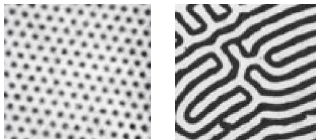


Figure 2: Type-II and intermediate type-II state (Brandt & Essmann, 1987).

- Due to high conductivity, the magnetic flux cannot be expelled from their interiors  $\Rightarrow$  neutron stars do not exhibit Meissner effect and are in a **metastable** state (Baym, Pethick & Pines, 1969; Ho, Andersson & Graber, 2017).

- State depends on **characteristic lengthscales** and standard considerations give  $\kappa = \lambda_*/\xi_{\text{ft}} > 1/\sqrt{2}$  in the outer core, i.e., a **type-II state** with

$$H_{c1} = 4\pi\mathcal{E}_{\text{ft}}/\phi_0 \sim 10^{14} \text{ G}, \quad H_{c2} = \phi_0/(2\pi\xi_{\text{ft}}^2) \sim 10^{15} \text{ G}. \quad (1)$$

- Each fluxtube carries a **flux quantum**  $\phi_0 = hc/2e \approx 2.1 \times 10^{-7} \text{ G cm}^2$ . All flux quanta add up to the total magnetic flux, so that the **averaged magnetic induction** is related to the fluxtube area density  $\mathcal{N}_{\text{ft}}$ :

$$B = \mathcal{N}_{\text{ft}}\phi_0, \quad \rightarrow \quad \mathcal{N}_{\text{ft}} \approx 4.8 \times 10^{18} (B/10^{12} \text{ G}) \text{ cm}^{-2}. \quad (2)$$

- Our understanding of **macroscopic NS superconductivity** is mainly based on **time-independent equilibrium** and **single-component** considerations.
- It is unclear what happens in the **stellar interior at different densities** as the star cools below  $T_c$  and when entrainment is included  $\Rightarrow$  how can we better understand the **SC phase** and its formation?
- Focus on the **two-condensate aspect** and expand on **earlier works** by Alpar, Langer & Sauls (1984); Charbonneau & Zhitnitsky (2007); Alford & Good (2008); Kobayakov et al. (2015); Haber & Schmitt (2017).

Rely on techniques for laboratory systems to construct **phase diagrams** of the protons by deducing their ground state in the presence of a magnetic field as a function of density.



- With entrainment, **velocity-dependent terms** in energy density read

$$F_{\text{vel}} = \frac{1}{2}\rho_p|\mathbf{V}_p|^2 + \frac{1}{2}\rho_n|\mathbf{V}_n|^2 - \frac{1}{2}\rho^{pn}|\mathbf{V}_p - \mathbf{V}_n|^2, \quad (3)$$

where  $\rho_p$  and  $\rho_n$  are the true mass densities, the coefficient  $\rho^{pn} < 0$  determines the strength of entrainment (Andreev & Bashkin, 1975) and  $\mathbf{V}_{p,n}$  are superfluid velocities related to canonical momenta, i.e.,  $\propto \nabla \arg \psi_x$ .

- In a mean-field framework, entrainment first enters at 4th order in  $\psi_{n,p}$  and 2nd order in their derivatives, i.e., we require a linear combination of

$$|\psi_x|^2|\nabla\psi_y|^2, \psi_x\psi_y\nabla\psi_x^* \cdot \nabla\psi_y^*, \psi_x\psi_y^*\nabla\psi_x^* \cdot \nabla\psi_y, \psi_x^*\psi_y^*\nabla\psi_x \cdot \nabla\psi_y, \quad (4)$$

where  $x, y \in \{p, n\}$ . Galilean invariance can be used to simplify the sum and is crucial to link our energy density to **nuclear physics models**.

- Total Helmholtz free energy density is obtained by adding entrainment terms to the usual free energy of a two-component superconductor, and introducing the magnetic vector potential  $\mathbf{A}$  by **minimal coupling**:

$$\begin{aligned}
 F[\psi_p, \psi_n, \mathbf{A}] = & F_0 - \mu_p |\psi_p|^2 - \mu_n |\psi_n|^2 + \frac{g_{pp}}{2} |\psi_p|^4 + \frac{g_{nn}}{2} |\psi_n|^4 + g_{pn} |\psi_p|^2 |\psi_n|^2 \\
 & + \frac{\hbar^2}{4m_u} \left| \left( \nabla - \frac{2ie}{\hbar c} \mathbf{A} \right) \psi_p \right|^2 + \frac{\hbar^2}{4m_u} |\nabla \psi_n|^2 + \frac{1}{8\pi} |\nabla \times \mathbf{A}|^2 \\
 & + h_1 \left| \left( \nabla - \frac{2ie}{\hbar c} \mathbf{A} \right) (\psi_n^* \psi_p) \right|^2 + \frac{1}{2} (h_2 - h_1) \nabla(|\psi_p|^2) \cdot \nabla(|\psi_n|^2) \\
 & + \frac{1}{4} h_3 \left( |\nabla(|\psi_p|^2)|^2 + |\nabla(|\psi_n|^2)|^2 \right), \quad (5)
 \end{aligned}$$

where  $F_0$  is an arbitrary reference level and proton Cooper pairs have charge  $2e$ .  $\mu_p$  and  $\mu_n$  are the chemical potentials, while  $g_{pp}$  and  $g_{nn}$  define the self-repulsion of the condensates, and  $g_{pn}$  their mutual repulsion.

- We connect this functional to the **Skyrme interaction** to obtain coefficients  $h_i$  that allow a **realistic description** of the neutron star interior:

$$h_1 = C_0^\tau - C_1^\tau, \quad h_2 = -4C_0^{\Delta\rho} + 4C_1^{\Delta\rho}, \quad (6)$$

$$h_3 = h_4 = C_0^\tau + C_1^\tau - 4C_0^{\Delta\rho} - 4C_1^{\Delta\rho}. \quad (7)$$

- The parameter  $h_1$  controls the entrainment (Chamel & Haensel, 2006)

$$\rho^{\text{pn}} = -\frac{2}{\hbar^2} h_1 \rho_n \rho_p. \quad (8)$$

- We also use the Skyrme model to determine the **stellar composition** (solving for baryon conservation, charge neutrality, beta equilibrium and muon production rate) (Chamel, 2008), but a separate **parametrisation** for the **SF/SC gaps** (Andersson, Comer & Glampedakis, 2005; Ho et al., 2015).

- To find the **ground state** in the presence of an **imposed magnetic field**, we can control (i) the magnetic flux density,  $\mathbf{B} = \nabla \times \mathbf{A}$ , by imposing a mean flux  $\bar{B}$ , or (ii) the thermodynamic external magnetic field  $\mathbf{H}$ .
- Case (i) approximates the **neutron star interior**, which becomes superconducting as the star cools in the presence of a pre-existing field.

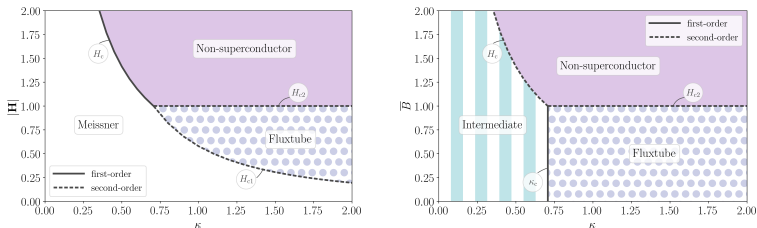


**Figure 3:** Phase diagrams for a one-component superconductor, for different values of the Ginzburg-Landau parameter,  $\kappa$ . The experiment with an imposed external field,  $|\mathbf{H}|$ , in nondimensional units is shown on the left, while the right panel shows the phase transitions in the experiment with an imposed mean flux,  $\bar{B}$ .

- We solve the Euler-Lagrange equations with **quasi-periodic boundary conditions** (Wood et al., 2019), which involves specifying the domain size  $L_x \times L_y$ , and the number  $N$  of magnetic flux quanta within the domain  $\Rightarrow$  different choices allow comparing **square** and **hexagonal lattices**.
- The Helmholtz free energy per magnetic flux quantum per unit length is

$$\mathcal{F} \equiv \frac{1}{N} \int_{x=0}^{L_x} \int_{y=0}^{L_y} F \, dx \, dy. \quad (9)$$

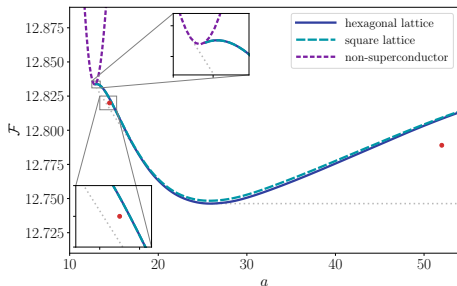


Figure 4: Helmholtz free energy per flux quantum per unit length,  $\mathcal{F}$ , as a function of the area per magnetic flux quantum,  $a = 2\pi/\bar{B}$ , for the NRAPR EoS at  $n_b = 0.2831/\text{fm}^3$ . The energy in the square (long-dashed, cyan) and hexagonal (solid, blue) lattice states matches smoothly onto the energy of the non-superconducting state (short-dashed, purple) at  $a \simeq 12.9$ .

- Choosing a sufficiently large domain, and values of  $a$ , we obtain examples of **inhomogeneous ground states**  $\Rightarrow$  for NRAPR at  $n_b = 0.2831/\text{fm}^3$  with  $a = 14.5$  plus  $N = 24$  (left) and  $a = 52$  plus  $N = 14$  (right).
- In both cases, the aspect ratio is  $\sqrt{3}$  and the **pure hexagonal lattice** a possible state but not the ground state  $\Rightarrow \mathcal{F}$  is lower than for pure lattice.

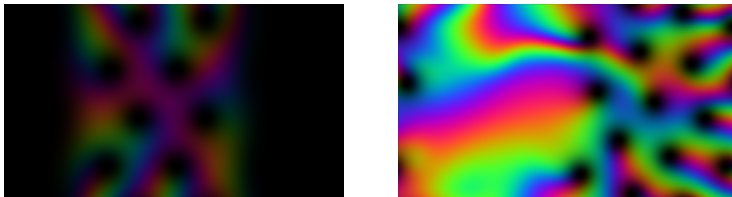


Figure 5: Inhomogeneous ground states for NRAPR. Brightness and hue indicate density and phase of the proton order parameter,  $\psi_p$ , respectively. The left panel shows a mixture of non-superconducting protons and hexagonal fluxtube lattice, while the right one is mixture of Meissner state and hexagonal fluxtube lattice.

- When such mixed states are present, second-order phase transitions are replaced by **first-order transitions** at  $H_{c1'} < H_{c1}$  and  $H_{c2'} > H_{c2}$ .
- We can determine **critical fields** (partially semi-analytically, partially numerically) and construct phase-diagrams of the superconducting state throughout the neutron star core. For the **LNS** equation of state:

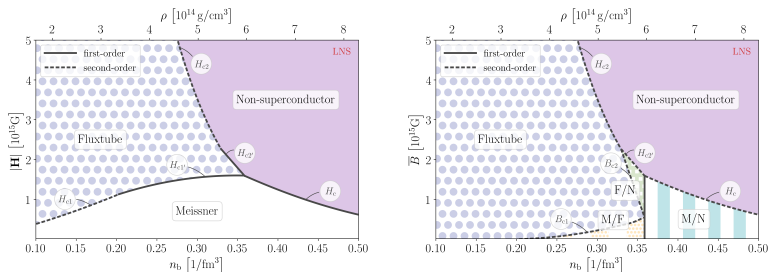
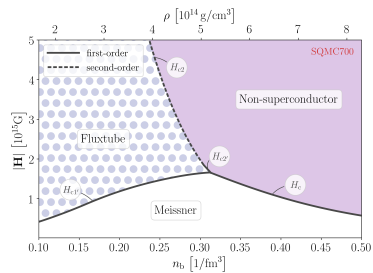
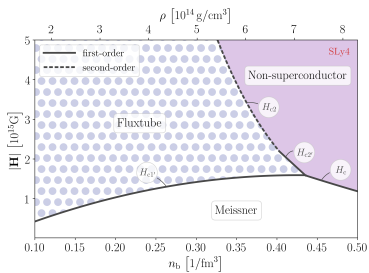
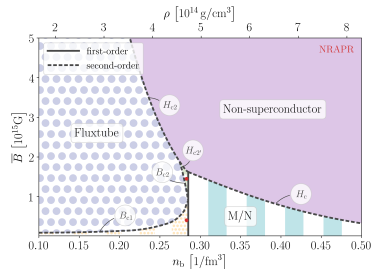
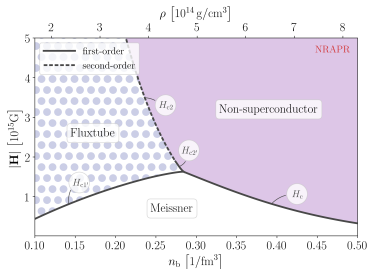
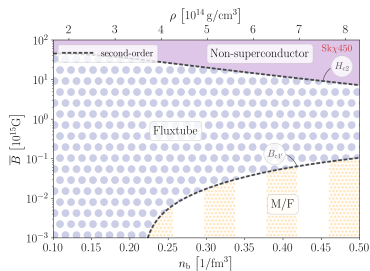
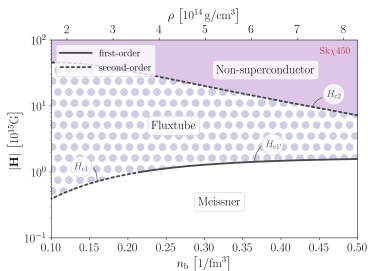
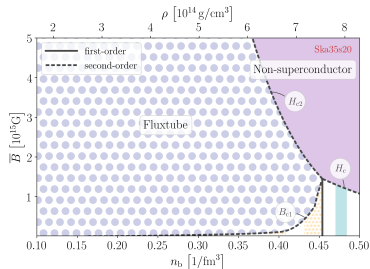
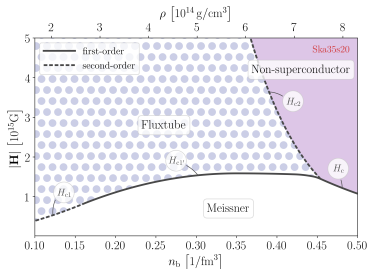


Figure 6: Phase diagrams for LNS. There are inhomogeneous regimes of the Meissner/Non-superconducting (M/N), Meissner/Fluxtube (M/F) and Fluxtube/Non-superconducting (F/N) states.







- Entrainment causes **type-1.5 SC** due to fluxtube repulsion on short scales and attraction on large scales  $\Rightarrow$  when imposing  $\bar{B}$ , mixed states appear.
- For typical EoSs, the outer core of pulsars with  $\lesssim 10^{14}$  G is not a type-II superconductor but mainly a type-1.5 system, where **magnetic flux is irregularly distributed and retained**.
- In the inner core, flux is distributed in an **intermediate type-I state**. The transition can be estimated via:

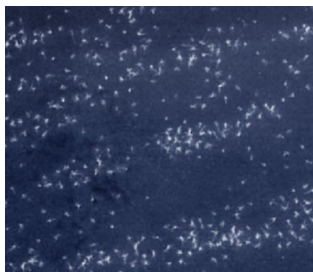
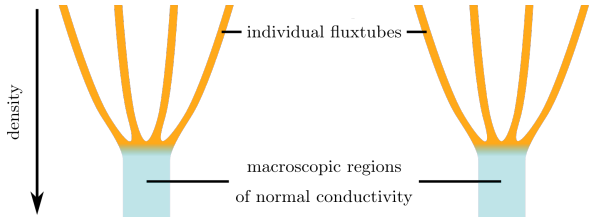
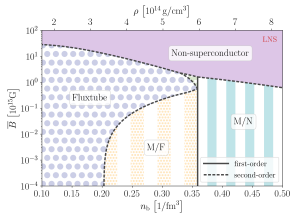


Figure 7: Magnetic decoration image of multi-band superconductor Mg<sub>2</sub>B (Moshchalkov et al., 2009).

$$\frac{\lambda_{\star}}{\xi_{\text{ft}}} = \frac{1}{\sqrt{2}} \sqrt{1 + h_1 \frac{n_n}{n_p}}. \quad (10)$$

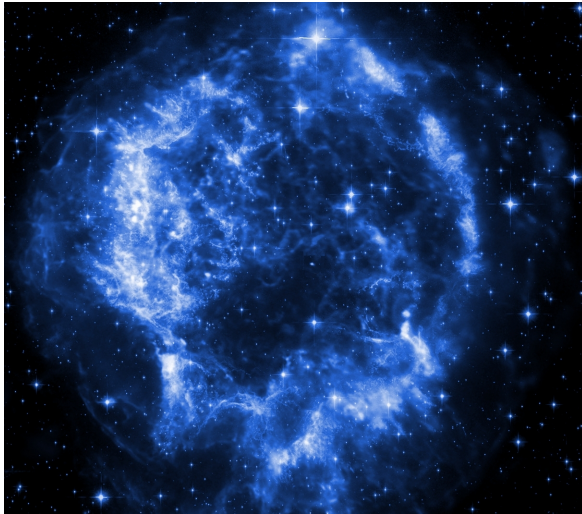


**Figure 8:** Zoomed-out version of the LNS phase diagram for a fixed mean flux (left). Schematic representation of the magnetic flux at the transition from outer to inner core (right).

- At low densities, protons are in a **type-1.5 regime**, where flux is quantized into thin fluxtubes (orange) of preferred separation (overall confined to a small fraction of the total volume).
- In the **type-I inner core**, flux is contained in macroscopic regions of normal conductivity (light blue) that alternate with flux-free regions.

- We assume that the **Skyrme model** correctly describes interactions up to the neutron star centre. If exotic particles / non-nucleonic matter are present, this would modify the picture at high densities.
- Our Ginzburg–Landau model is **time-independent** and neglects **rotation**, i.e., we do not capture dynamics or incorporate neutron vortices, which are crucial to get the full macroscopic picture.
- For a full dynamical model, we would need to incorporate the **electron component**. However, they are **normal** and do not form a quantum condensate. We do not have a formalism to consistently include such a (particle) component in the Ginzburg–Landau model.

# The end



- To find the **ground state** for our system in the presence of an **imposed magnetic field**, we can perform two distinct experiments: we control (i) the magnetic flux density,  $\mathbf{B} = \nabla \times \mathbf{A}$ , by imposing a mean or net magnetic flux, or (ii) the thermodynamic external magnetic field,  $\mathbf{H}$ .
- In the first case, we minimise the **Helmholtz free energy**,  $\mathcal{F} = \langle F \rangle$ , where the angled brackets represent some kind of integral over our physical domain  $\Rightarrow$  closely approximates the conditions in the neutron star core, which becomes superconducting as the star cools in the presence of pre-existing magnetic field. The ground state can be **inhomogeneous**.
- In the second case, we minimise the dimensionless **Gibbs free energy**,  $\mathcal{G} = \mathcal{F} - 2\kappa^2 \mathbf{H} \cdot \langle \mathbf{B} \rangle$ . In an unbounded domain, the ground state is guaranteed to be **homogeneous**, and the phase diagram simpler.

- Whether we work with  $\mathcal{F}$  or  $\mathcal{G}$ , we obtain the same equations of motion:

$$\kappa^2 \nabla \times (\nabla \times \mathbf{A}) = \Im \left\{ \psi_p^* (\nabla - i\mathbf{A}) \psi_p + \frac{h_1}{\epsilon} \psi_n \psi_p^* (\nabla - i\mathbf{A}) (\psi_n^* \psi_p) \right\}, \quad (11)$$

$$\begin{aligned} \nabla^2 \psi_n &= R^2 (|\psi_n|^2 - 1) \psi_n + \alpha (|\psi_p|^2 - 1) \psi_n \\ &\quad - h_1 \psi_p (\nabla + i\mathbf{A})^2 (\psi_p^* \psi_n) \\ &\quad - \psi_n \nabla^2 \left( \frac{h_2 - h_1}{2} |\psi_p|^2 + \frac{h_3}{2\epsilon} |\psi_n|^2 \right), \end{aligned} \quad (12)$$

$$\begin{aligned} (\nabla - i\mathbf{A})^2 \psi_p &= (|\psi_p|^2 - 1) \psi_p + \frac{\alpha}{\epsilon} (|\psi_n|^2 - 1) \psi_p \\ &\quad - \frac{h_1}{\epsilon} \psi_n (\nabla - i\mathbf{A})^2 (\psi_n^* \psi_p) \\ &\quad - \psi_p \nabla^2 \left( \frac{h_2 - h_1}{2\epsilon} |\psi_n|^2 + \frac{h_3}{2} |\psi_p|^2 \right). \end{aligned} \quad (13)$$

- $F$  is approximated numerically on a regular 2D grid. The order parameters  $\psi_p$  and  $\psi_n$  are defined on the gridpoints as  $\psi_p^{i,j}$  and  $\psi_n^{i,j}$ , while the vector field  $\mathbf{A}$  has two components,  $(A_x, A_y)$ , defined on the corresponding links between the gridpoints, i.e., we have  $A_x^{i+1/2,j}$  and  $A_y^{i,j+1/2}$ .
- The gauge coupling between  $\psi_p$  and  $\mathbf{A}$  is implemented using a **Peierls substitution** to preserve (discrete) gauge symmetry, e.g.,

$$\begin{aligned} \left| \left( \frac{\partial}{\partial x} - iA_x \right) \psi_p \right| &= \left| \frac{\partial}{\partial x} \exp(-\int iA_x dx) \psi_p \right| \\ \Rightarrow \left| \left( \frac{\partial}{\partial x} - iA_x \right) \psi_p \right|^{i+1/2,j} &\simeq \frac{1}{\delta x} \left| \exp(-iA_x^{i+1/2,j} \delta x) \psi_p^{i+1,j} - \psi_p^{i,j} \right|. \end{aligned} \quad (14)$$

- This leads to a discrete approximation  $\mathcal{F}_{\text{dis}}[\psi_p^{i,j}, \psi_n^{i,j}, A_x^{i+1/2,j}, A_y^{i,j+1/2}]$  and we obtain the ground state using a gradient-descent, iteration method.



- In the outer core, initially, only protons are superconducting (neutrons remain normal), so we model the **formation of the superconducting phase** with a single-component time-dependent Ginzburg-Landau model.
- Study the **dynamics of the phase transition** under different circumstances in analogy to numerical experiments of laboratory systems (Liu, Mondello & Goldenfeld, 1991; Frahm, Ullah & Dorsey, 1991).

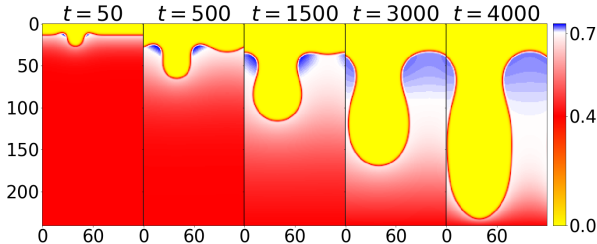


Figure 9: Evolution of the magnetic field in a type-I system in the nucleation regime.

- Alford M. G., Good G., 2008, *Physical Review B*, 78, 024510
- Alpar M. A., Langer S. A., Sauls J. A., 1984, *The Astrophysical Journal*, 282, 533
- Andersson N., Comer G., Glampedakis K., 2005, *Nuclear Physics A*, 763, 212
- Andreev A. F., Bashkin E. P., 1975, *Soviet Physics JETP*, 42, 164
- Baym G., Pethick C. J., Pines D., 1969, *Nature*, 224, 673
- Chamel N., 2008, *Monthly Notices of the Royal Astronomical Society*, 388, 737
- Chamel N., Haensel P., 2006, *Physical Review C*, 73, 045802
- Charbonneau J., Zhitnitsky A. R., 2007, *Physical Review C*, 76, 015801
- Frahm H., Ullah S., Dorsey A. T., 1991, *Physical Review Letters*, 66, 3067
- Haber A., Schmitt A., 2017, *Physical Review D*, 95, 116016
- Ho W. C., Glampedakis K., Andersson N., 2012, *Monthly Notices of the Royal Astronomical Society*, 422, 2632
- Ho W. C. G., Elshamouty K. G., Heinke C. O., Potekhin A. Y., 2015, *Physical Review C*, 91, 015806
- Ho W. W. C. G., Andersson N., Graber V., 2017, *Physical Review C*, 96, 065801
- Kobyakov D. N., Samuelsson L., Marklund M., Lundh E., Bychkov V., Brandenburg A., 2015, arXiv preprint
- Liu F., Mondello M., Goldenfeld N., 1991, *Physical Review Letters*, 66, 3071
- Moshchalkov V. V. et al., 2009, *Physical Review Letters*, 102, 117001
- Steiner A. W., Prakash M., Lattimer J. M., Ellis P. J., 2005, *Physics reports*, 411, 325
- Wood T. S., Mesgarnezhad M., Stagg G. W., Barengi C. F., 2019, *Physical Review B*, 100, 024505